Conventional dendritic cells regulate the outcome of colonic inflammation independently of T cells

Kazumichi Abe*, Kim Phung Nguyen*, Sean D. Fine*, Ji-Hun Mo*, Carol Shen*, Steve Shenouda*, Maripat Corr*, Steffen Jung†, Jongdae Lee*, Lars Eckmann*, and Eyal Raz*‡

*Department of Medicine, University of California at San Diego, La Jolla, CA 92093; and †Department of Immunology, Weizmann Institute of Science, Rehovot 76100, Israel

We explored the physiological role of conventional dendritic cells (cDCs) in acute colitis induced by a single cycle of dextran sodium sulfate administration. Depending on their mode of activation and independently of T cells, cDCs can enhance or attenuate the severity of dextran sodium sulfate-induced colitis. The latter beneficial effect was achieved, in part, by IFN-1 induced by Toll-like receptor 9-activated cDCs. IFN-1 inhibits colonic inflammation by regulating neutrophil and monocyte trafficking to the inflamed colon and restraining the inflammatory products of tissue macrophages. These data highlight a novel role of cDCs in the regulation of other innate immune cells and position them as major players in acute colonic inflammation.

colitis | Toll-like receptor 9 | IFN-1

Different models of experimental colitis have been instrumental in defining the fundamental mechanisms and cellular interplay that lead to colonic inflammation (1, 2). Acute colitis induced by a single cycle of dextran sodium sulfate (DSS) administration is characterized by mucosal ulceration and submucosal inflammation provoked by a disrupted epithelial barrier and subsequent translocation of luminal microbiota into the lamina propria (LP) (1, 2).

Toll-like receptors (TLRs) are crucial sensors of the innate immune system that recognize signature microbial compounds (3, 4). Although intestinal microbiota, under certain conditions, provokes intestinal inflammation, it also supports colonic homeostasis mainly via TLR signaling (5–7). In addition to innate immune cells such as macrophages (Macs) or dendritic cells (DCs), intestinal epithelial cells express a spectrum of TLRs (8). However, the contribution of TLR-activated DCs to colonic homeostasis or colonic inflammation is yet unknown. We and others recently observed that the systemic administration of certain TLR ligands, especially TLR9 ligand, effectively reduces the severity of colonic inflammation in DSS and other models of experimental colitis (6, 9–11). When used in a preventive mode, administration of TLR9 (10) or TLR3 (12) ligands ameliorates DSS-induced colitis mainly via the induction of IFN-1.

As DCs are the major cellular source of IFN-1 induced by TLR signaling, we sought to uncover and define their regulatory role in colonic homeostasis by using both diphtheria toxin (DT)-induced ablation of conventional DCs (cDCs) (i.e., CD11c^hi) in tg-DTR mice (13) and adoptive transfer approaches. Here, we present evidence that depending on their mode of activation, cDCs either enhance or inhibit acute DSS-induced colitis independently of T cells. The inhibition of colitis in this model was caused, in part, by IFN-1 production by cDCs that regulates the recruitment of neutrophils and monocytes and the inflammatory activities of tissue Macs in the inflamed colon.

Results

Depletion of cDCs Suppresses Acute Colitis Induced by a Single-Cycle Administration of DSS.
To investigate the role of cDCs in colonic inflammation, we used DT-mediated depletion of cDCs in tg-DTR mice (13, 14). In preliminary studies we optimized the conditions for depletion of cDCs [supporting information (SI) Fig. 5 A and B]. Administration of DT over 2 successive days depleted >97% of cDCs (SI Fig. 5C) in tg-DTR mice. Neither plasmacytoid DCs nor Macs were affected by DT injection (SI Fig. 5 D). As most of the parameters of acute colitis are observed in the last 2 days of DSS administration, we reasoned that the coinciding depletion of cDCs might provide a tool to investigate their major effector functions.

The injection of DT into WT mice did not influence the outcome of DSS-induced colitis (SI Fig. 6A). We then tested whether depletion of cDCs affects the acute colitis induced by a single cycle of DSS administration. To our surprise, cDC depletion significantly suppressed DSS-induced colitis, as reflected by the disease activity index (DAI) and histological score (HS) (Fig. 1A and B). Histological analysis revealed that cDC depletion attenuated mucosal ulceration (Fig. 1D) and neutrophil infiltration (Fig. 1 E and F). Accordingly, colon explants from DSS-treated and cDC-depleted mice produced few proinflammatory cytokines (TNF-α, IL-6, and IL-12) compared with those from the DSS-treated group without cDC depletion (Fig. 1G).

Depletion of cDCs in TLR9 Ligand-Treated Mice Aggravates DSS-Induced Colitis.
Activation of TLR9 by its ligand [immunostimulatory sequence (ISS)-oligodeoxynucleotide (ODN), also known as CpG-ODN], when used in a preventive mode, inhibited acute colitis induced by DSS in tg-DTR mice similar to what we and others have previously reported in WT mice (9–11). Depletion of cDCs, however, abolished the antiinflammatory effects of TLR9 activation as measured by the DAI and HS (Fig. 2 A and B). Depletion of cDCs also reversed the ISS-mediated amelioration of weight loss, which occurred between days 6 and 7 (Fig. 2C), and ISS-mediated attenuation of mucosal ulceration (Fig. 2D). Notably, a significant increase in the infiltration of neutrophils was seen in the LP after cDC depletion (Fig. 2 E and F). Consistent with these data, higher levels of proinflammatory cytokines (TNF-α, IL-6, and IL-12) were detected in the supernatants of colonic explants from cDC-depleted mice (15) (Fig. 2G).

Regulation of DSS-Induced Colitis by cDCs Is Independent of T Cells.
We recently demonstrated that the administration of TLR9 ligand inhibits acute colitis induced by a single cycle of DSS
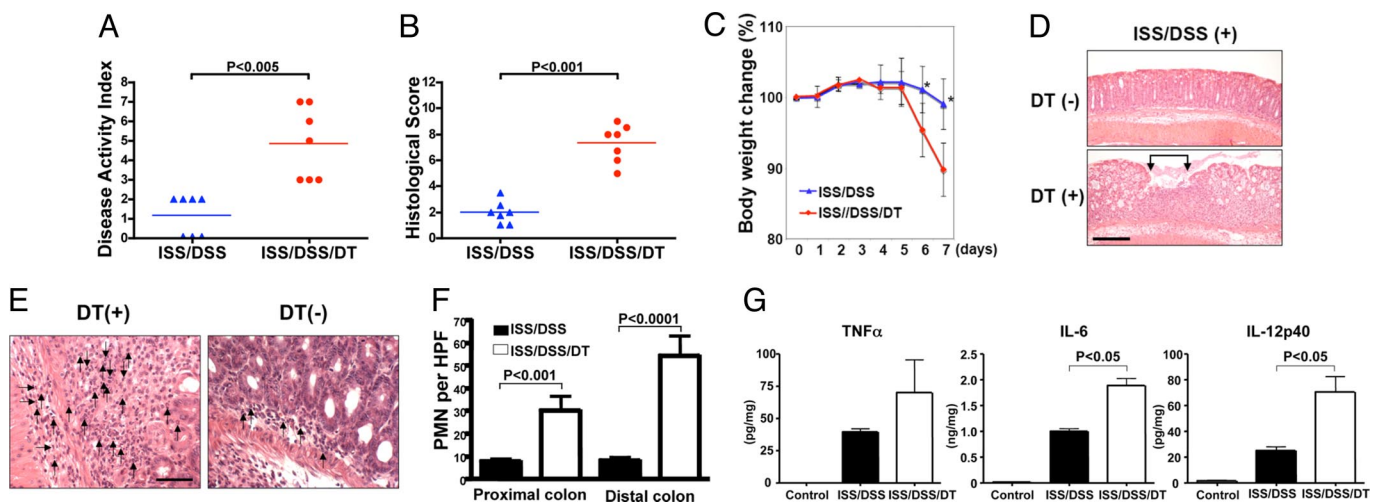

Fig. 1. Depletion of cDCs suppresses DSS-induced colitis. tg-DTR mice were given DSS for 7 days, injected with DT or PBS i.p. on days 5 and 6, and analyzed on day 7 as described in *Materials and Methods*. (*A*) DAI. (*B*) HS. (*C*) All mice were weighed daily, and data are presented as mean body weight ± SD. *, *P* < 0.05. (*D*) Histological evaluation of colon. Paraffin sections of colons from tg-DTR mice (*n* = 7 mice per group), treated as indicated, were prepared and stained with H&E. Ulcerated areas are indicated by arrows. (Scale bar: 10 μm.) (*E*) Photomicrographs of representative areas from DSS- and DSS/DT-treated mice as indicated. Arrows highlight PMN infiltrates. (Scale bar: 5 μm.) (*F*) PMNs per HPF were counted in the proximal and distal colons of DSS- and DSS/DT-treated tg-DTR mice (*n* = 7 mice per group). *P* values were calculated by Mann–Whitney test. (*G*) Freshly isolated colon explants were cultured for 24 h in complete RPMI medium 1640, and cytokine release was measured by ELISA. Results represent mean cytokine levels (± SD; pg/mg colonic tissue) in samples. Data are representative of two independent experiments.

administration in RAG−/− mice (10) that lack B and T cells. To evaluate whether the results obtained above for tg-DTR mice could be reproduced in RAG−/− mice, we intercrossed tg-DTR to RAG−/− mice and then injected DT to DSS- and ISS/DSS-treated tg-DTR/RAG−/− mice under the same conditions specified above for tg-DTR mice. The depletion of cDCs in these immune-deficient mice resulted in changes in the DAI and HS (SI Fig. 6 *B and C*) similar to those observed in the immune-competent tg-DTR mice (Figs. 1*A* and 2*A*).

As the depletion of cDCs, with or without prior ISS-ODN

administration, resulted in either a proinflammatory or an antiinflammatory phenotype, respectively (Figs. 1*A* vs. 2*A* and SI Fig. 6 *B* vs. *C*), we concluded that the mode of cDC activation determines their phenotype, which, in turn, dictates the outcome of colonic inflammation independently of T cells.

Distinct Cytokine Expression Determines the Contrasting Phenotypes of cDCs. To further explore the antiinflammatory and proinflammatory cDC phenotypes, we compared the transcript levels of cytokines in the cDCs isolated from the spleen (SP) and colonic LP

Fig. 2. Depletion of cDCs in TLR9 ligand-treated mice aggravates DSS-induced colitis. tg-DTR mice were injected with PBS or ISS-ODN (10 μg per mouse) s.c. 2 h before DSS administration. On days 5 and 6, mice were injected with DT or PBS and analyzed on day 7 as described in *Materials and Methods*. (*A*) DAI. (*B*) HS. (*C*) All mice were weighed daily, and data are presented as mean body weight ± SD. *, *P* < 0.05. (*D*) Histological evaluation of colon. Paraffin sections of the colon from tg-DTR mice (*n* = 7 mice per group), treated as indicated, were prepared and stained with H&E. Ulcerated areas are indicated by arrows. *P* values were calculated by Mann–Whitney test. (Scale bar: 10 μm.) (*E*) Photomicrographs of representative areas from ISS/DSS- and ISS/DSS/DT-treated mice as indicated. Arrows highlight PMN infiltrates. (Scale bar: 5 μm.) (*F*) PMNs per HPF were counted in the proximal colon and distal colon of ISS/DSS- and ISS/DSS/DT-treated tgDTR mice (*n* = 7 mice per group). *P* values were calculated by Mann–Whitney test. (*G*) Freshly isolated colon explants from mice were cultured 24 h in complete RPMI medium 1640, and cytokine release was measured by using ELISA. Results represent mean cytokine levels (± SD; pg/mg colonic tissue) in samples. Data are representative of two independent experiments.
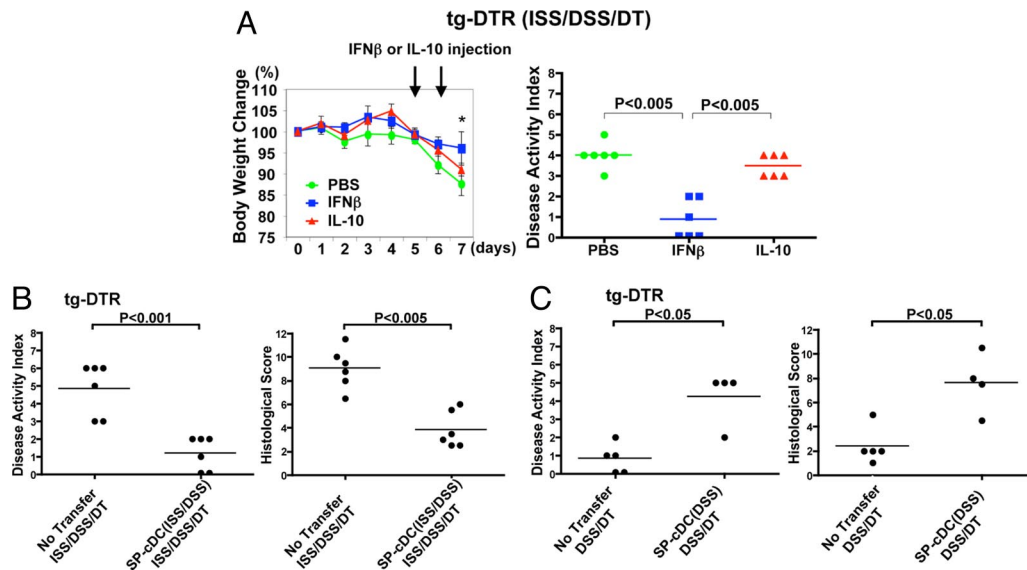
Fig. 3. Administration of rIFN-β or adoptive transfer of cDCs reverses the outcome of colitis. ISS/DSS-treated tg-DTR mice were injected i.p. with mouse rIFN-β (1,000 units per mouse per day), mouse IL-10 (1 μg per mouse per day), or PBS on days 5 and 6 of DT administration. (*A*) Change in body weight (data presented as mean body weight ± SD; *, $P < 0.05$) and DAI. (*B*) SP-cDCs were isolated on day 5 from ISS/DSS-treated B6 mice as described in *Materials and Methods* and were adoptively transferred i.p. into ISS/DSS-treated tg-DTR mice (2×10^5 cells per mouse) on the fifth day of DSS administration. DT was injected on days 5 and 6. Colitis was evaluated on day 7 of DSS administration. (*C*) SP-cDCs were isolated on day 5 from DSS-treated B6 mice and were adoptively transferred i.p. into DSS-treated tg-DTR mice (2×10^5 cells per mouse) on the fifth day of DSS administration. DT was injected on days 5 and 6. Colitis was evaluated on day 7 after DSS administration. *P* values were calculated by Mann–Whitney test and were representative of two independent experiments ($n = 4$–6 mice per group).

of WT mice before or after treatment with either DSS or ISS/DSS. Whereas cDCs from the SP or LP of ISS/DSS-treated mice produced IFN-β mRNA, cDCs from DSS-treated mice did not (SI Fig. 7*A*). IL-10 transcript levels showed a trend similar to that observed for IFN-β (SI Fig. 7 *B and C*). In contrast to IFN-β and IL-10, the transcript levels of the proinflammatory cytokines (TNF-α and IL-6) were higher in cDCs isolated from DSS-treated mice than in ISS/DSS-treated mice (SI Fig. 7 *B and C*) possibly because of some non-cDC within the isolated LP-cDC population.

We next examined whether IFN-1 induction pathways are differentially activated in the antiinflammatory and proinflammatory cDC phenotypes. Consistent with the IFN-β mRNA data, the levels of the IFN regulatory factor (IRF)-1 and IRF-7 activation were significantly higher in SP-cDCs isolated from ISS/DSS-treated mice compared with SP-cDCs isolated from DSS-treated mice (SI Fig. 7*D*).

Administration of Recombinant IFN-β (rIFN-β), but Not Recombinant IL-10 (rIL-10), Reverses the Outcome of Colitis in ISS/DT/DSS-Treated Mice. Our data suggest that the inhibition of colitis by TLR9-activated cDCs might be largely caused by IFN-1 or IL-10 produced by these cells (SI Fig. 7 *A and B*). To further clarify which of these two cytokines inhibits colonic inflammation, rIFN-β or rIL-10 was administered to ISS/DT/DSS-treated tg-DTR mice on days 5 and 6. These days, and not others, were chosen to match the depletion of the cDCs in the tg-DTR mice. Thus, their administration in the cDC-depleted animals could provide a clue as to which cDC-derived cytokine mediates the beneficial effect in this model. Indeed, as presented in Fig. 3*A*, systemic administration of rIFN-β attenuated colonic inflammation. In contrast, the administration of rIL-10, under the specified experimental conditions, did not have any effect. The latter observation is supported by our previous study (6) that demonstrated that administration of ISS-ODN is effective in reducing colitis indices in IL-10$^{-/-}$ mice treated with DSS.

Adoptive Transfer of cDCs Reverses the Colitis Phenotype Provoked by DT Administration. To test whether the two types of cDCs described above can transport their regulatory functions to another

animal, we transferred SP-cDCs isolated from ISS/DSS-treated WT mice to ISS/DSS/DT-treated tg-DTR mice. Indeed, the transfer of SP-cDCs isolated from ISS/DSS-treated WT mice attenuated colonic inflammation induced by cDC depletion in ISS/DT/DSS-treated tg-DTR mice (Fig. 3*B*). In contrast, when SP-cDCs isolated from DSS-treated WT mice were adoptively transferred to DT/DSS-treated tg-DTR mice, they reversed the attenuation of colitis achieved upon cDC depletion (Fig. 3*C*).

IFN-1 Accelerates the Resolution of Acute Colitis Induced by DSS Administration. We have previously demonstrated the antiinflammatory effects of IFN-1 (a TLR9-induced product) in DSS-induced colitis (10), but the related mechanisms are still unclear. As IFN-1 regulates the expression of different chemokines (16), we hypothesized that IFN-1 advances the resolution of inflammation by differential recruitment of neutrophils and monocytes into inflamed colon. Indeed, IFN-α/βR$^{-/-}$ mice displayed a significant delay in body weight gain 1 week after the withdrawal of DSS as compared with WT mice (Fig. 4*A*) and reached their pre-DSS body weight 1 week after WT mice did (i.e., day 21; data not shown). This observation correlated with the cellular infiltrates seen in the LP. Whereas neutrophils were dominant in IFN-α/βR$^{-/-}$ mice, F4/80-positive Macs dominated the WT colonic LP during the recovery phase (Fig. 4*B*). Consistent with these findings, KC (17, 18), a neutrophil-attracting chemokine, was produced at significantly higher levels in the supernatants of colonic explants from IFN-α/βR$^{-/-}$ than from WT mice (Fig. 4*C*), whereas RANTES (19), a monocyte/Mac-attracting chemokine, was detected at higher levels in WT than in IFN-α/βR$^{-/-}$ colonic explants (Fig. 4*C*).

Conventional DCs Down-Regulate the Proinflammatory Profile of Tissue Macs. The depletion of cDCs in ISS/DSS/DT-treated tg-DTR mice enhanced the severity of colonic inflammation (Fig. 2). These data suggest that ISS-stimulated cDCs restrain the inflammatory activity of other cell types upon DSS administration. We hypothesized that tissue Mac might contribute to colonic inflammation in ISS/DSS/DT-treated mice. To validate
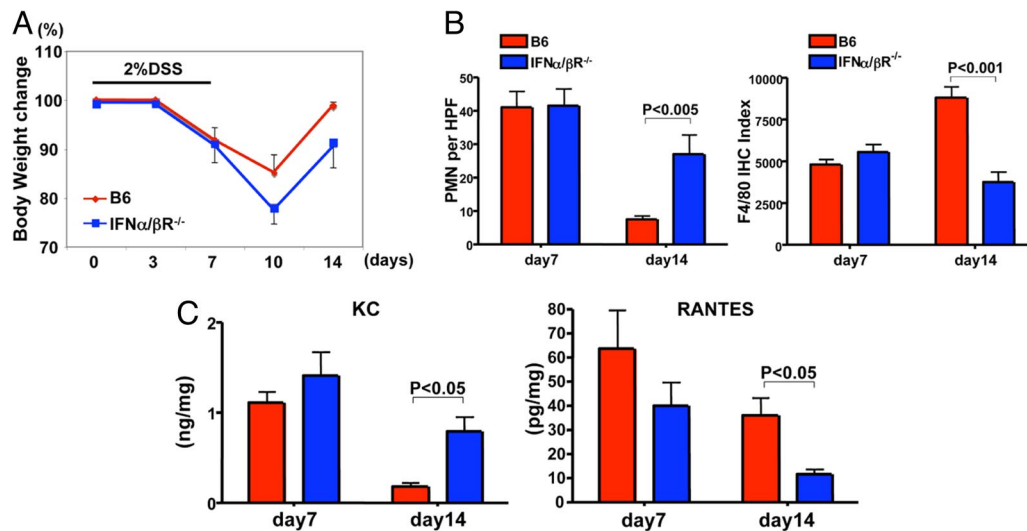
Fig. 4. IFN-1 accelerates the resolution of colonic inflammation. (*A*) B6 (WT) and IFN-α/βR$^{-/-}$ mice were given DSS for 7 days and analyzed on days 7 and 14 as described in *Materials and Methods*. All mice were weighed on days 0, 3, 7, 10, and 14. Data are presented as mean body weight $\pm$ SD, $n = 4$ mice per group. (*B*) PMN and Mac (F4/80+) count per HPF in the distal colon on days 7 and 14 after DSS treatment in WT(B6) or IFN-α/βR$^{-/-}$ (B6) mice. *P* values were calculated by Mann–Whitney test. (*C*) Freshly isolated colon explants from mice were cultured 24 h in complete RPMI medium 1640, and cytokine release in the supernatants was measured by Luminex. Results represent mean chemokine levels ($\pm$ SD; pg/mg or ng/mg colonic tissue) in samples. Data are representative of two independent experiments.

the potential inflammatory role of Macs in experimental colitis, we first transferred WT bone marrow-derived DCs (BMDCs, i.e., bona fide cDCs), or WT bone marrow-derived Mac (BMDM) that had been stimulated or unstimulated with ISS-ODN *in vitro*, before their transfer to recipient DSS-treated WT mice. Indeed, the transfer of ISS-stimulated, but not unstimulated, BMDCs attenuated DSS-induced colitis (SI Fig. 8*A*). In contrast, the transfer of ISS-stimulated, but not unstimulated, BMDMs exacerbated DSS-induced colitis (SI Fig. 8*B*).

To further investigate a potential regulatory function of cDCs on tissue Macs, we isolated mRNA from SP-Mac and LP-Mac from DSS-treated tg-DTR mice that were injected with ISS-ODN with or without depletion of cDCs (SI Fig. 9 *A* and *B*). The transcript levels of proinflammatory cytokines such as TNF-α, IL-1β, and IL-12p40 and chemokines such as MIP1-α, MIP1-β, and CXCL1 (KC) were significantly increased in ISS-treated SP-Mac after cDC depletion and were augmented even further in LP-Mac under the same conditions (SI Fig. 9*B*). To investigate whether antiinflammatory cytokines produced by cDCs suppress the proinflammatory profiles of SP-Mac and LP-Mac, we i.p.-injected the cDC-derived antiinflammatory cytokines identified above (SI Fig. 7), i.e., rIFN-β or rIL-10, to ISS/DSS-treated tg-DTR mice after cDCs were depleted. We then measured the change in the expression levels of proinflammatory mediators in the adjacent tissue Mac. As presented in SI Fig. 9 *C* and *D*, the injection of rIFN-β, or rIL-10 to a lesser extent, suppressed the expression of some proinflammatory mediators in tissue Mac. Taken together, these results support the notion that cDCs restrain the proinflammatory and colitogenic activities of ISS-stimulated Mac, but they do not rule out a proinflammatory role for another cell type, in this model of experimental colitis.

Discussion

Different types of hematopoietic cells contribute to colonic inflammation induced by a single cycle of DSS administration. However, whatever is the contribution of a particular cell to this process, our study indicates that the extent and severity of colonic inflammation are determined by cDCs. These cells have a dual function in our experimental system. As presented in Fig. 1, the depletion of cDCs in DSS-treated tg-DTR mice almost

completely inhibited experimental colitis (i.e., the proinflammatory phenotype of cDCs), whereas the depletion of cDCs in ISS/DSS-treated animals enhanced colonic inflammation (i.e., the antiinflammatory phenotype of cDCs; see Fig. 2). This regulatory role of cDCs is most likely the result of their special ability to generate, receive, integrate, and transmit a variety of biological signals. Because of their localization in the LP, cDCs can affect the functionality of intestinal epithelial cells, stromal cells, and blood-derived cells (neutrophils, Macs, and plasma-cytoid dendritic cells). In this respect, cDCs function as the central processor and a key effector of colonic homeostasis.

The acute colitis induced by a single cycle of DSS administration is a T cell-independent inflammatory reaction. It is characterized by colonic epithelial-cell death (e.g., ulcer), mucosal edema, and, consequently, the accumulation of neutrophils that is necessary to limit bacterial translocation to the adjacent tissue. Subsequently, phagocytic monocytes and Macs accumulate to remove dead cells (e.g., neutrophils) and tissue debris and help to restore the physiologic function of the inflamed mucosa (20). Our previous (10) and current analyses have identified that TLR-induced IFN-1 facilitates the resolution of DSS-induced colitis. We noticed that whereas polymorphonuclear neutrophils (PMNs) dominated the cellular infiltrate in the acute phase (Fig. 1 *D* and *E*), monocytes/Macs dominated the infiltrate in the resolution phase of colitis (Fig. 4*C*). Consistent with these results, the neutrophil chemoattractant KC (17, 18) was produced at higher levels by IFN-α/βR$^{-/-}$ than WT colons (Fig. 4*C*), whereas the monocyte chemoattractant RANTES (19) was produced at higher levels in WT than IFN-α/βR$^{-/-}$ colons.

Our results underline the pivotal function of cDCs in colonic homeostasis and define their role as the cellular switch that regulates this type of colonic inflammation. Depending on their mode of activation, cDCs (*i*) secrete a variety of inflammatory cytokines (SI Fig. 7), (*ii*) secrete antiinflammatory cytokines that inhibit both their own and Mac-produced inflammatory cytokines (SI Figs. 7 and 8), and (*iii*) regulate the production of certain chemokines that dictate the composition of the cellular infiltrate (Fig. 4) and, consequently, affect the pace of resolution of the inflamed colon.

IMMUNOLOGY

Recent studies have proposed a T cell-independent regulation of Macs by DCs. DCs, when cultured *in vitro* with IL-10 and TGF-β, produced antiinflammatory mediators and suppressed the production of proinflammatory mediators induced by LPS-activated Macs (21). The observation that depletion of cDCs after ISS-ODN administration enhanced the proinflammatory expression profile in SP-Mac and LP-Mac, and that this proinflammatory profile is reinhibited in this setting by rIFN-β administration, further suggests that the regulation of tissue Mac by cDCs is largely mediated by this cytokine (SI Fig. 8). However, our data do not rule out a proinflammatory role for another cell type, provoked upon cDC depletion, in this model of experimental colitis.

Collectively, these data expand the role of cDCs beyond T cell activation and position cDCs as important regulators of acute inflammation. We propose that interventions aimed at inducing regulatory DCs may benefit patients with a variety of inflammatory diseases.

Materials and Methods

Reagents. The following materials were obtained from commercial sources: DSS (30–50 kDa) (ICN, Aurora, OH); hemoccult, (Beckman Coulter, Franklin Lakes, NJ); primers (Integrated DNA Technologies, Coralville, IA); SuperScript First-Strand Synthesis system for RT-PCR (Invitrogen, Carlsbad, CA); 96-well Optical Reaction Plate (Applied Biosystems, Foster City, CA); DT (D-0564; Sigma, St. Louis, MO); mouse rIFN-β (Chemicon International, Temecula, CA); mouse rIL-10 (BD PharMingen, San Diego, CA); ISS-ODN [1018, TLR9-L, 5'-TGACTGTG<u>AACGTTCG</u>AGATGA-3'; TriLink BioTechnologies (10)]. Underline indicates the active motif.

Mice. Specific-pathogen-free C57BL/6 (B6), RAG1$^{-/-}$, and B6.FVB-Tg (Itgax-DTR/EGFP)57Lan/J (tg-DTR) mice ages 6–10 weeks were purchased from The Jackson Laboratory (Bar Harbor, ME). B6.FVB-Tg(Itgax-DTR/EGFP)57Lan/J and RAG1$^{-/-}$ mice were intercrossed (tg-DTR/RAG$^{-/-}$) and bred in our vivarium at the University of California at San Diego. IFN-α/βR$^{-/-}$ mice were backcrossed to the B6 background for 10 generations in our vivarium. All experimental procedures were conducted in accordance with the University of California at San Diego institutional guidelines for animal care and use. For systemic DC depletion, tg-DTR mice were injected i.p. with 100 ng DT per mouse in PBS on days 5 and 6 of DSS administration.

Evaluation of Acute Colitis Induced by DSS. Mice on the B6 background were given 1.5–2% (wt/vol) DSS dissolved in sterile, distilled water ad libitum for 7 days (i.e., one cycle of DSS). Groups of mice were treated with 10 μg of ISS-ODN per mouse, s.c., 2 h before DSS administration. The DAI (the combined score of weight loss and bleeding) was determined as described (6, 9, 10).

Histological Scoring. Histological scoring of H&E-stained colonic tissues was performed as described (10). PMNs per high-power field (HPF) were counted in the proximal and distal colon ($n = 7$).

Quantification of Immunohistochemical Staining. Colons were dissected and fixed with Bouin's solution (Sigma) and embedded in paraffin. Five-micrometer sections were prepared, deparaffinized, and stained with anti-F4/80 antibody. Avidin (0.1%) was added and incubated for 15 min followed by incubation with 0.01% biotin for 15 min and incubation with anti-mouse F4/80 antibody (Serotec, Raleigh, NC) overnight at room temperature. Slides were then washed and incubated with Mayer Hematoxylin solution for 5 min. Using Photoshop, version 9.0, software (Adobe Systems, Mountain View, CA), 10 fields per slide were

Table 1. Primers and sequences used

RT-PCR primer	Sequence
CPH	F-5'-ATGGTCAACCCCACCGTGT-3'
	R-5'-TTCTTGCTGTCTTGGAACTTTGTC-3'
TNF-α	F-5'-ATGATCCCAGCCACCCGCTCGCTTCTC-3'
	R-5'-TTACTTGGGGACACCTTTTAGCATCTT-3'
IL-1β	F-5'-GAAGAAGAGCCCATCCTCTG-3'
	R-5'-TCATCTCGGAGCCTGTAGTG-3'
IL-6	F-5'-GACTGATGCTGGTGACAACC-3'
	R-5'-CCTCCGACTTGTGAAGTGG-3'
IL-12p40	F-5'-AAACCAGACCCGCCCAAGAAC-3'
	R-5'-AAAAAGCCAACCAAGCAGAAGACAG-3'
IL-23p19	F-5'-TCCGTTCCAAGATCCTTCG-3'
	R-5'-GAACCTGGGCATCCTTAAGC-3'
IL-10	F-5'-TGCACTACCAAAGCCACAAAGCAG-3'
	R-5'-TCAGTAAGAGCAGGCAGCATAGCA-3'
TGF-β	F-5'-AGCAACATCACACAAGACAGACT-3'
	R-5'-TTAGAAGGGGCCGTGGCGAAACAG-3'
IFN-β	F-5'-TCAGCTGCACTTGCACTTGCAGGAGCGCACAAT-3'
	R-5'-GATACCAACTATTGCTTCAGCTCCACA-3'
IL-1Ra	F-5'-GTCTTGTGCCAAGTCTGGAG-3'
	R-5'-AGAGCGGATGAAGGTAAAGC-3'
MIP-1α	F-5'-GACAAGCTCACCCTCTGTCA-3'
	R-5'-AGAAGAACAGCAAGGGCAGT-3'
MIP-1β	F-5'-AAGCCAGCTGTGGTATTCCT-3'
	R-5'-CTCTCCTGAAGTGGCTCCTC-3'
CXCL1	F-5'-ACCCAAACCGAAGTCATAGC-3'
	R-5'-GTGCCATCAGAGCAGTCTGT-3'
MMP9	F-5'-CATTCGCGTGGATAAGGAGT-3'
	R-5'-TCACACGCCAGAAGAATTTG-3'

evaluated for F4/80 staining so as to best reflect the overall immunostaining of colon tissue (22).

Isolation of cDCs (CD11c^{hi}) and Macs from SP. SPs were removed, cut into small pieces, and digested in RPMI media 1640 containing 10% FCS, antibiotics, 300 units/ml collagenase II (Worthington, Lakewood, NJ), and 20 μg/ml DNase I (Worthington) with magnetic stirrer for 15 min. The digested tissue was then passed through a cell strainer, and the digestion was repeated once more. The DC population was initially enriched by discontinuous density gradient centrifugation using OptiPrep (Sigma) according to the manufacturer's instruction. Low-density cells at the interface were then harvested. cDCs (defined as CD11c^{hi} B220$^-$) were isolated by the removal of B220$^+$ cells by using B220 MicroBeads followed by positive selection with CD11c MicroBeads (23). Macs (defined as CD11b$^+$ CD11c$^-$ B220$^-$) were isolated by the removal of CD11c$^+$ B220$^+$ Thy-1.2$^+$ cells using CD11c, B220, and Thy-1.2 MicroBeads followed by positive selection with CD11b MicroBeads (Miltenyi Biotec, Auburn, CA) (24).

Isolation of cDCs and Macs from Colonic LP. Briefly, colons were removed, split lengthwise, and washed three times in cold PBS with 1 mM DTT (Sigma) to discard luminal contents. To remove epithelium, colons were incubated with shaking in Hanks' balanced salt solution containing 5 mM EDTA, 10 mM Hepes, and 0.05 mM DTT at 37°C, for 60 min. To isolate DCs, colons were digested in RPMI media 1640 containing 10% FCS, 300 units/ml collagenase A (Roche, Indianapolis, IN), and 20 μg/ml DNase I (Worthington) with a magnetic stirrer for 30 min. The digested tissue was then passed through a cell strainer, and the digestion was repeated once more. After OptiPrep (Sigma) density centrifugation at $600 \times g$ for 15 min, cells at the high- and low-density interfaces were harvested. CD11c^{hi} cells (cDC) (25)

and CD11b$^+$ (Mac) cells were enriched by positive selection using MACS MicroBeads, according to the manufacturer's protocol (Miltenyi Biotec).

In Vitro Stimulation of BMDMs and BMDCs. BMDMs and BMDCs from B6 mice were prepared as described (26). CD11c^{hi} cells were isolated by positive selection using MACS MicroBeads, according to the manufacturer's protocol (Miltenyi Biotec). For stimulation of cells, BMDMs or BMDCs (1×10^6 cells/ml) were incubated with or without ISS-ODN (10 μg/ml) for 4 h.

Adoptive Transfer. For adoptive transfer-based experiments, SP-cDCs (2×10^5 cells per mouse) were transferred i.p. into DSS-treated tg-DTR mice (recipient) on the fifth day of DSS administration (2% DSS in the drinking water for 7 days). Recipient mice were injected with DT (100 ng per mouse) i.p. on days 5 and 6. In another experimental setting, *in vitro* ISS-stimulated or unstimulated BMDCs (2×10^6 cells per mouse) or BMDMs (2×10^6 cells per mouse) were transferred i.p. into DSS-treated B6 mice on the fifth day of DSS administration. Colitis was evaluated as described above.

FACS Analysis. Briefly, single cell suspensions were aliquoted and nonspecific sites were blocked with FcBlock (PharMingen) followed by labeling with the following fluorescent-conjugated antibodies: FITC anti-CD11b and FITC anti-B220 (PharMingen), phycoerythrin (PE) anti-CD11b (PharMingen), PE anti-F4/80 (Serotec), PE anti-mPDCA (Miltenyi Biotec), and allophycocyanin anti-CD11c (PharMingen). Cells were acquired on a FACS Caliber cytometer (BD Biosciences) and analyzed by using FlowJo software (Tree Star, Ashland, OR).

Quantitative RT-PCR. Messenger RNA isolation using a MicroFast Track mRNA isolation kit (Invitrogen), reverse transcription, conventional PCR, and real-time PCR were carried out following standard methods as described (6). The RT-PCR primers (see Table 1) specific for target genes were designed based on their reported sequences by using the Primer 3 program (http://fokker.wi.mit.edu/primer3/input.htm) and synthesized by IDT Technologies (Coralville, IA). Quantitative real-time PCR was performed on an AB 7300 (Applied Biosystems, Warrington, U.K.) using SYBR GREEN PCR Master Mix (Applied Biosystems). Amplification conditions were: 50°C (2 min), 95°C (10 min), 40 cycles of 95°C (15 s), and 60°C (60 s).

The expression of each mRNA was normalized to CPH expression, calculated as $2^{(Ct[CPH]-Ct[gene])}$, and compared with the levels of mRNA obtained in untreated mice (27).

Measurement of Cytokine Protein Levels in Intestinal Tissues. Tissues from the midcolon were isolated and rinsed in Hanks' balanced salt solution, weighed, and cut into 5-mm segments. Colonic explants were cultured overnight in 48-well tissue culture plates (Costar, Corning, NY) in 500 μl of complete RPMI medium 1640 at 37°C in an atmosphere containing 5% CO_2. After centrifugation to pellet and remove debris, culture supernatants were collected and stored at −20°C. Cytokine concentrations were measured by ELISA (TNF-α, IL-6, and IL-12) or Luminex (KC and RANTES; Bio-Rad, Hercules, CA) and were normalized to the weight of each colonic explant.

Signaling Assays. Nuclear extracts were prepared from SP-cDCs isolated from DSS-treated or ISS/DSS-treated B6 (WT) mice. Levels of different IRFs in the nuclei were measured before and after stimulation by using nuclear extracts of SP-cDCs. IRFs were detected by Western blotting (28) using antibodies specific for IRF-1 (Santa Cruz Biotechnology, Santa Cruz, CA), IRF-3, and IRF-7 (Invitrogen). Activation of STAT1 was evaluated with antibodies specific for phosphorylated STAT1 (29) (Cell Signaling Technology, Beverly, MA). Levels of β-actin (Sigma–Aldrich, St. Louis, MO) were used for normalization of protein loading.

1. Powrie F, Uhlig H (2004) *Novartis Found Symp* 263:164–174; discussion 174-178 and 211–218.
2. Strober W, Fuss IJ, Blumberg RS (2002) *Annu Rev Immunol* 20:495–549.
3. Akira S (2003) *J Biol Chem* 278:38105–38108.
4. Beutler JZ, Georgel P, Crozat K, Croker B, Rutschmann S, Du X, Hoebe K (2006) *Annu Rev Immunol* 24:354–389.
5. Abreu MT, Fukata M, Arditi M (2005) *J Immunol* 174:4453–4460.
6. Rachmilewitz D, Karmeli F, Takabayashi K, Hayashi T, Leider-Trejo L, Lee J, Leoni LM, Raz E (2002) *Gastroenterology* 122:1428–1441.
7. Rakoff-Nahoum S, Paglino J, Eslami-Varzaneh F, Edberg S, Medzhitov R (2004) *Cell* 118:229–241.
8. Lee J, Mo JH, Katakura K, Alkalay I, Rucker AN, Liu YT, Lee HK, Shen C, Cojocaru G, Shenouda S, *et al.* (2006) *Nat Cell Biol* 8:1327–1336.
9. Rachmilewitz D, Katakura K, Karmeli F, Hayashi T, Reinus C, Rudensky B, Akira S, Takeda K, Lee J, Takabayashi K, Raz E (2004) *Gastroenterology* 126:520–528.
10. Katakura K, Lee J, Rachmilewitz D, Li G, Eckmann L, Raz E (2005) *J Clin Invest* 115:695–702.
11. Obermeier F, Dunger N, Strauch UG, Grunwald N, Herfarth H, Scholmerich J, Falk W (2003) *Clin Exp Immunol* 134:217–224.
12. Vijay-Kumar M, Wu H, Aitken J, Kolachala VL, Neish AS, Sitaraman SV, Gewirtz AT (2007) *Inflamm Bowel Dis* 13:856-864.
13. Jung S, Unutmaz D, Wong P, Sano G, De los Santos K, Sparwasser T, Wu S, Vuthoori S, Ko K, Zavala F, *et al.* (2002) *Immunity* 17:211–20.
14. Vallon-Eberhard A, Landsman L, Yogev N, Verrier B, Jung S (2006) *J Immunol* 176:2465–2469.
15. Hue S, Ahern P, Buonocore S, Kullberg MC, Cua DJ, McKenzie BS, Powrie F, Maloy KJ (2006) *J Exp Med* 203:2473–2483.
16. Padovan E, Spagnoli GC, Ferrantini M, Heberer M (2002) *J Leukocyte Biol* 71:669–676.
17. Matsukawa A, Hogaboam CM, Lukacs NW, Lincoln PM, Strieter RM, Kunkel SL (1999) *J Immunol* 163:6148–6154.
18. Zhang XW, Liu Q, Wang Y, Thorlacius H (2001) *Br J Pharmacol* 133: 413–421.
19. Lotan D, Zilberman D, Dagan O, Keller N, Ben-Abraham R, Weinbroum AA, Harel R, Barzilay Z, Paret G (2001) *Ann Thorac Surg* 71:233–237.
20. Serhan CN, Brain SD, Buckley CD, Gilroy DW, Haslett C, O'Neill LA, Perretti M, Rossi AG, Wallace JL (2007) *FASEB J* 21:325–332.
21. Fujita S, Seino K, Sato K, Sato Y, Eizumi K, Yamashita N, Taniguchi M, Sato K (2006) *Blood* 107:3656–3664.
22. Lehr HA, Mankoff DA, Corwin D, Santeusanio G, Gown AM (1997) *J Histochem Cytochem* 45:1559–1565.
23. Hayashi T, Beck L, Rossetto C, Gong X, Takikawa O, Takabayashi K, Broide DH, Carson DA, Raz E (2004) *J Clin Invest* 114:270–279.
24. Nomura T, Kawamura I, Tsuchiya K, Kohda C, Baba H, Ito Y, Kimoto T, Watanabe I, Mitsuyama M (2002) *Infect Immun* 70:1049–1055.
25. Niess JH, Brand S, Gu X, Landsman L, Jung S, McCormick BA, Vyas JM, Boes M, Ploegh HL, Fox JG, *et al.* (2005) *Science* 307:254–258.
26. Martin-Orozco E, Kobayashi H, Van Uden J, Nguyen MD, Kornbluth RS, Raz E (1999) *Int Immunol* 11:1111–1118.
27. Livak KJ, Schmittgen TD (2001) *Methods* 25:402–408.
28. Au WC, Pitha PM (2001) *J Biol Chem* 276:41629–41637.
29. Hsu LC, Park JM, Zhang K, Luo JL, Maeda S, Kaufman RJ, Eckmann L, Guiney DG, Karin M (2004) *Nature* 428:341–345.

IMMUNOLOGY